Orthograde dihydropyridine receptor signal regulates ryanodine receptor passive leak

José Miguel Eltit[a,1], Hongli Li[a,2], Christopher W. Ward[b], Tadeusz Molinski[c], Isaac N. Pessah[d], Paul D. Allen[a,3], and José R. Lopez[a]

[a]Department of Anesthesiology, Perioperative and Pain Medicine, Brigham and Women's Hospital, Boston, MA 02115; [b]School of Nursing, University of Maryland, Baltimore, MD 21201; [c]Department of Chemistry and Biochemistry and Skaggs School of Pharmacy and Pharmaceutical Sciences, University of California at San Diego, La Jolla, CA 92093; and [d]Department of Molecular Biosciences, School of Veterinary Medicine, University of California at Davis, Davis, CA 95616

Edited* by Clara Franzini-Armstrong, University of Pennsylvania Medical Center, Philadelphia, PA, and approved March 24, 2011 (received for review December 17, 2010)

The skeletal muscle dihydropyridine receptor (DHPR) and ryanodine receptor (RyR1) are known to engage a form of conformation coupling essential for muscle contraction in response to depolarization, referred to as excitation–contraction coupling. Here we use WT and $Ca_V1.1$ null (dysgenic) myotubes to provide evidence for an unexplored RyR1–DHPR interaction that regulates the transition of the RyR1 between gating and leak states. Using double-barreled Ca^{2+}-selective microelectrodes, we demonstrate that the lack of $Ca_V1.1$ expression was associated with an increased myoplasmic resting $[Ca^{2+}]$ ($[Ca^{2+}]_{rest}$), increased resting sarcolemmal Ca^{2+} entry, and decreased sarcoplasmic reticulum (SR) Ca^{2+} loading. Pharmacological control of the RyR1 leak state, using bastadin 5, reverted the three parameters to WT levels. The fact that Ca^{2+} sparks are not more frequent in dysgenic than in WT myotubes adds support to the hypothesis that the leak state is a conformation distinct from gating RyR1s. We conclude from these data that this orthograde DHPR-to-RyR1 signal inhibits the transition of gated RyR1s into the leak state. Further, it suggests that the DHPR-uncoupled RyR1 population in WT muscle has a higher propensity to be in the leak conformation. RyR1 leak functions are to keep $[Ca^{2+}]_{rest}$ and the SR Ca^{2+} content in the physiological range and thus maintain normal intracellular Ca^{2+} homeostasis.

L-type calcium channel | resting calcium

In skeletal muscle the free cytosolic Ca^{2+} concentration at rest ($[Ca^{2+}]_{rest}$) is ≈120 nM, and the concentration found in the extracellular space and in intracellular stores is in the millimolar range (1). This enormous chemical gradient of Ca^{2+} ions is crucial because all of the Ca^{2+} signaling processes in living cells are based in spatial and temporally controlled Ca^{2+} transients (2). Understanding how cells maintain cytoplasmic Ca^{2+} homeostasis at $[Ca^{2+}]_{rest}$ under normal and pathophysiological conditions can provide essential information about muscle disorders, including muscular dystrophies (3), central core disease/malignant hyperthermia (4, 5), and inclusion body myositis (6, 7).

It is currently thought that the sarco-endoplasmic Ca^{2+} ATPase, the plasma membrane Ca^{2+} ATPase, and the Ca^{2+}/Na^{+} exchanger of the plasma membrane regulate the myoplasmic Ca^{2+} concentration in skeletal muscle (2, 8). However, it has also been demonstrated that resting sarcolemmal Ca^{2+} entry and "passive" sarcoplasmic reticulum (SR)-Ca^{2+} leak are working simultaneously, opposing mechanisms that exclude Ca^{2+} from the cytosol. As a result the homeostatic $[Ca^{2+}]_{rest}$ is set by a fine and complex equilibrium among influx and efflux pathways regulating Ca^{2+} ions (9–13).

The physical coupling between the dihydropyridine receptor (DHPR) and the ryanodine receptor (RyR1) is essential for skeletal excitation–contraction coupling, engaging a form of bidirectional signaling. During orthograde signaling, sarcolemmal depolarization elicits conformational changes in $Ca_V1.1$ that are physically transmitted to RyR1 channels, promoting their opened state. Through retrograde signaling, RyR1 increases the L-type current of the DHPR (14). Freeze-fracture images have shown that DHPRs are clustered in groups of four particles (tetrads), which owing to steric hindrance are associated with alternate RyR1s in each Ca^{2+} release unit. Thus, alternate RyR1 channels are not physically coupled with DHPRs. It is known that the coupled DHPR/RyR1 channels engage retrograde as well as orthograde coupling, but the function of the uncoupled RyR1 population is unknown (15–17).

We have previously shown that a significant part of the Ca^{2+} leak pathway from the SR is ryanodine insensitive, arising from a constitutively open ($P_O \approx 1$) low conductance conformation of RyR1. This ryanodine-insensitive conformation is distinct from the actively gating ryanodine-sensitive conformation that is involved in excitation-contraction coupling (10, 18). Bastadin 5 (B5), a brominated macrocyclic derivative of dityrosine isolated from the marine sponge *Iathella basta* (19), interacts with RyR1, modulating RyR1 gating behavior in a FKBP12-dependent manner. B5 can be used as a pharmacological tool to convert RyR1 from its leak conformation into a gating conformation (19).

In the present study, we identify a previously undiscovered orthograde signal from the DHPR to RyR1 that dictates the ratio of actively gating RyR1 channels vs. those in the leak conformation, thus setting resting myoplasmic Ca^{2+} concentration. Using double-barreled Ca^{2+}-selective microelectrodes, we demonstrate that dysgenic myotubes, which lack expression of $Ca_V1.1$, have increased $[Ca^{2+}]_{rest}$, higher resting Ca^{2+} entry, and decreased SR Ca^{2+} loading compared with WT cells. Pharmacological control of RyR1 leak state, using B5, equalizes all three parameters between WT and dysgenic myotubes. We conclude that a previously unreported orthograde DHPR/RyR1 signaling significantly inhibits the transition of RyR1 into the RyR1 leak state, keeping the $[Ca^{2+}]_{rest}$ and the SR Ca^{2+} content in the physiological range. In addition, our work suggests that the RyR1 population not coupled to the DHPR in WT muscle has a higher propensity to be in the leak conformation and thus may be determinant in maintaining normal intracellular Ca^{2+} homeostasis.

Author contributions: J.M.E., I.N.P., P.D.A., and J.L. designed research; J.M.E., H.L., C.W.W., and J.L. performed research; T.M. contributed new reagents/analytic tools; J.M.E., H.L., C.W.W., and J.L. analyzed data; and J.M.E., C.W.W., I.N.P., P.D.A., and J.L. wrote the paper.

The authors declare no conflict of interest.

*This Direct Submission article had a prearranged editor.

[1]Present address: Department of Physiology and Biophysics, School of Medicine, Virginia Commonwealth University, Richmond, VA 23298.

[2]Present address: Department of Histology, Third Military Medical University, Chongqing 400038, China.

[3]To whom correspondence should be addressed. E-mail: allen@zeus.bwh.harvard.edu.

This article contains supporting information online at www.pnas.org/lookup/suppl/doi:10.1073/pnas.1018380108/-/DCSupplemental.

Results

Dysgenic Myotubes Have a Higher $[Ca^{2+}]_{rest}$ than WT Cells. To determine the influence of the DHPR on the $[Ca^{2+}]_{rest}$ in myotubes, we measured it directly with Ca^{2+}-selective microelectrodes in differentiated WT and dysgenic ($Ca_V1.1$ null) myotubes. In agreement with previous studies (1, 10), $[Ca^{2+}]_{rest}$ in WT myotubes was 121 ± 1.7 nM (n = 18), but it was significantly elevated (163 ± 2.5 nM, n = 17; $P < 0.001$) in dysgenic myotubes (Fig. 1). To ascertain whether the absence of $Ca_V1.1$ was solely responsible for this difference, dysgenic cells were permanently transduced with $Ca_V1.1$ using lentiviral infection, and transduced myoblasts were cloned to ensure homogeneity of expression, as described in *Materials and Methods*. WT and transduced dysgenic myotubes (dysgenic+$Ca_V1.1$) express $Ca_V1.1$ when assessed by Western blotting and have the expected punctate pattern when tested by immunocytochemistry, showing clustering of DHPRs at the cell surface, presumably at sites of peripheral couplings (20). These clusters are absent in untransduced dysgenic myotubes (Fig. 2). This demonstrates that proper targeting of the protein. $[Ca^{2+}]_{rest}$ in dysgenic+$Ca_V1.1$ myotubes (119 ± 1.1 nM, n = 17) was not different from WT myotubes (Fig. 1), indicating that the difference in $[Ca^{2+}]_{rest}$ between dysgenic and WT cells was due to the absence of $Ca_V1.1$ in the former.

$[Ca^{2+}]_{rest}$ of Dysgenic Myotubes Is Normalized by Treatment with B5. Exposure to B5 resulted in decrease of $[Ca^{2+}]_{rest}$ to comparable values in all three types of myotubes. $[Ca^{2+}]_{rest}$ after treatment was 99 ± 0.7 nM (n = 16) in WT, 103 ± 1.3 nM (n = 16) in dysgenic, and 94 ± 2.2 nM (n = 10) in dysgenic+$Ca_V1.1$ myotubes (Fig. 1). As previously shown (19), the action of B5 requires an intact RyR1–FKBP12 complex. Pretreatment with FK506 to disrupt the RyR1–FKBP12 interaction caused a significant increase in $[Ca^{2+}]_{rest}$ to 139 ± 2.4 nM, 217 ± 3.0 nM, and 136 ± 1.3 nM (n = 10) in WT, dysgenic, and $Ca_V1.1$+dysgenic myotubes, respectively (Fig. 1). After this treatment, addition of B5 had no significant effect in lowering $[Ca^{2+}]_{rest}$ in any of the myotubes, the values remaining at 129 ± 1.8 nM, 202 ± 3.5 nM, and 133 ± 0.8 nM, respectively (n = 10; Fig. 1). These experiments clearly show that B5 treatment equalizes the resting $[Ca^{2+}]_{rest}$ in all of the three cell types and that pretreatment with FK506 abolishes this effect.

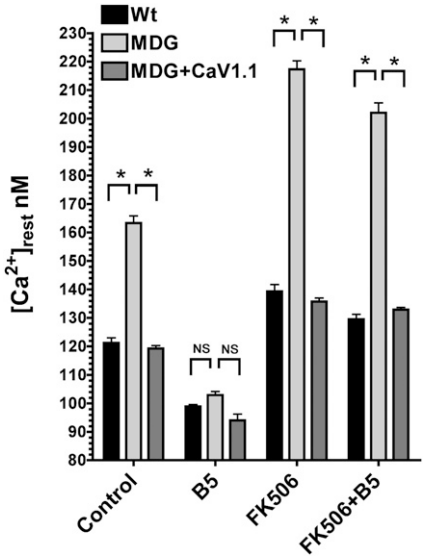

Fig. 1. B5 equalizes $[Ca^{2+}]_{rest}$ among $Ca_V1.1$-expressing and dysgenic (MDG) myotubes. $[Ca^{2+}]_{rest}$ determinations were done in WT (n = 18), dysgenic (MDG, n = 17), and dysgenic myotubes transduced with $Ca_V1.1$ lentivirus (MDG+$Ca_V1.1$, n = 16). Where indicated, the measurements were done in the presence of 20 μM B5 (WT n = 18, dysgenic n = 16, and dysgenic+$Ca_V1.1$ n = 10), FK506 (WT n = 10, dysgenic n = 10, and dysgenic+$Ca_V1.1$ n = 10), or FK506 plus B5 (FK506+B5, WT n = 10, dysgenic n = 10, and dysgenic+$Ca_V1.1$ n = 10). Mean ± SEM is shown. *$P < 0.001$ (ANOVA). NS, not significant.

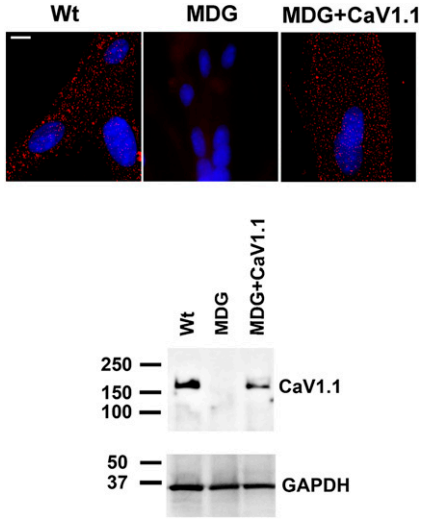

Fig. 2. Dysgenic (MDG) myotubes do not express the α1S subunit of the DHPR ($Ca_V1.1$). The expression of $Ca_V1.1$ was assessed by immunostaining in WT, dysgenic (MDG), and dysgenic (MDG)+$Ca_V1.1$ myotubes. Clusters of DHPRs (red foci) are located at the cell surface in WT and in dysgenic+$Ca_V1.1$ but not in dysgenic myotubes. Western blot confirms lack of $Ca_V1.1$ expression in dysgenic myotubes and its rescue by stable transduction. (Scale bar, 10 μm.)

Resting Ca^{2+} Entry Is Increased in Dysgenic Myotubes. Resting Ca^{2+} entry was estimated using Mn^{2+} quench technique as described in *Materials and Methods*. The rate of decay of the Fura-2 fluorescence was −0.485 ± 0.048 arbitrary units (a.u.)/s (n = 32) in WT myotubes but was significantly higher (0.677 ± 0.072 a.u./s, n = 25, $P < 0.01$) in dysgenic cells (Fig. 3*A*). To evaluate the contribution of passive Ca^{2+} entry to $[Ca^{2+}]_{rest}$, we used the Ca^{2+} entry blocker BTP2 (11, 21). After BTP2 (5 μM) pretreatment $[Ca^{2+}]_{rest}$ decreased from 117 ± 1.8 nM (n = 12) to 89 ± 1.8 nM (n = 10) in WT myotubes, and from 158 ± 2.0 nM (n = 11) to 121 ± 1.7 nM (n = 11) in dysgenic myotubes (Fig. 3*B*). Although BTP2 has a greater effect on dysgenic than WT myotubes, the blocking effect is not sufficient to equalize the difference in $[Ca^{2+}]_{rest}$ between the two genotypes (Fig. 3*B*). As before, B5 nullified the difference in $[Ca^{2+}]_{rest}$ between WT (99 ± 0.7 nM, n = 17) and dysgenic myotubes (102 ± 1.2 nM, n = 18), and further addition of BTP2 decreased $[Ca^{2+}]_{rest}$ to the same extent in both genotypes [79 ± 1.1 nM (n = 10) and 83 ± 0.9 nM (n = 10) in WT and dysgenic, respectively]. These data suggest that the reduction of RyR1 leak by the action of B5 may have an effect on SR Ca^{2+} content, which in turn signals entry pathways in the sarcolemma.

Dysgenic Myotubes Have Decreased SR-Ca^{2+} Content That Can Be Normalized with B5. To estimate the SR Ca^{2+} content, we loaded the cells with the low-affinity Ca^{2+} probe Fluo-5N and measured the increase in cytosolic fluorescence during a 20-mM caffeine challenge in absence of extracellular Ca^{2+} (1 mM EGTA). Interestingly WT myotubes always gave larger Ca^{2+} responses than dysgenic myotubes (Fig. 4). Analysis of the area under the curve shows that the Ca^{2+} released by caffeine was approximately fourfold smaller in dysgenic (25 ± 2.3 a.u., n = 69) vs. WT myotubes (107 ± 8.5 a.u., n = 66), despite the fact that

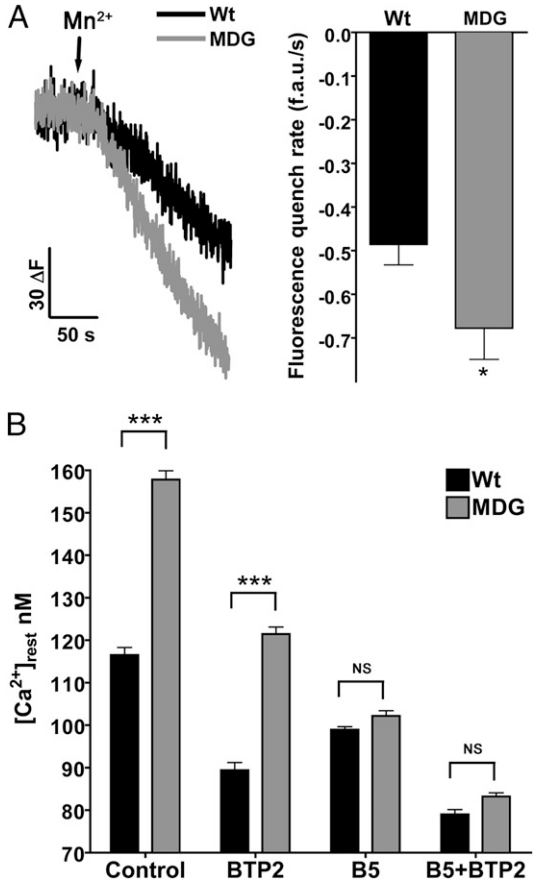

Fig. 3. Resting Ca^{2+} entry is increased in dysgenic myotubes. Resting Ca^{2+} entry was estimated using the Mn^{+2} quench technique. (*A*) Representative traces for WT and dysgenic are shown. The fluorescence decay induced by Mn^{2+} permeability was fitted to a linear regression for each response: WT (n = 32) and dysgenic (MDG) (n = 25). Mean ± SEM is shown. *$P < 0.05$ (t test). (*B*) $[Ca^{2+}]_{rest}$ was measured as described in *Materials and Methods*. The measurements were done in WT (n = 12) and dysgenic (MDG) myotubes (n = 11) in control conditions, treated with 5 μM BTP2 alone (WT n = 10, dysgenic n = 11), B5 alone (WT n = 17, dysgenic n = 18), or the combination of both drugs (B5+BTP2, WT n = 10, dysgenic n = 10). Results are shown as mean ± SEM. ***$P < 0.001$ (ANOVA). NS, not significant.

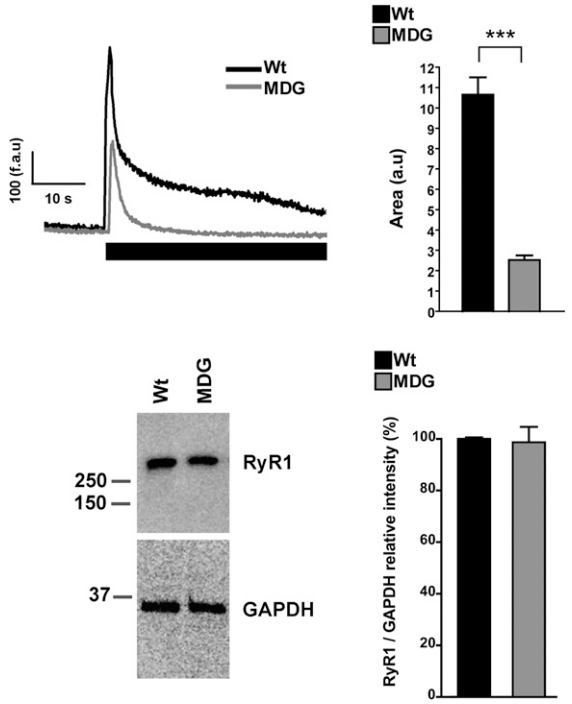

Fig. 4. Dysgenic myotubes have decreased releasable SR Ca^{2+}. WT and dysgenic myotubes loaded with Fluo-5N were exposed to 20 mM caffeine in free Ca^{2+} media (1 mM EGTA) as describes in *Materials and Methods*. Representative traces are shown for WT and dysgenic (MDG) myotubes; the black rectangle shows when caffeine was applied. The area under the curve of each response was calculated [WT n = 66 and dysgenic (MDG) n = 69], and the data are shown as mean ± SEM. ***$P < 0.001$ (ANOVA) (*Upper*). Western blot analysis shows that RyR1 expression is not different between WT and dysgenic myotubes [*Lower*; WT n = 3 and dysgenic (MDG) n = 3].

Western blot analysis showed the same level of RyR1 expression (Fig. 4). As a second approach to estimate the intracellular Ca^{2+} content, we loaded the cells with the ratiometric Ca^{2+} probe Fura-4F and measured the increase of cytosolic Ca^{2+} concentration while emptying the SR using the Ca^{2+} ionophore 4Br-A23187 (Fig. 5) in absence of extracellular Ca^{2+} (1 mM EGTA). Two parameters were calculated for each response: the peak value and the area under the curve. WT myotubes showed greater Ca^{2+} transients than dysgenic myotubes for both parameters: 2.1 ± 0.2 $ratio_{(340/380)}$ (n = 20) vs. 1.5 ± 0.1 $ratio_{(340/380)}$ (n = 29) peak values, and 30 ± 5.5 (a.u.) (n = 20) vs. 18 ± 1.9 (a.u.) (n = 29) area values, respectively. B5 treatment had no significant effect on either parameter in WT myotubes but normalized the Ca^{+2} content in dysgenic myotubes to WT levels [2.3 ± 0.2 $ratio_{(340/380)}$ (n = 15) dysgenic vs. 2.3 ± 0.1 $ratio_{(340/380)}$ (n = 24) WT peak values, and 30 ± 4.4 (a.u.) (n = 15) dysgenic and 30 ± 1.7 (a.u.) (n = 24) WT area] (Fig. 5).

Increased $[Ca^{2+}]_{rest}$ in Dysgenic Myotubes Is Not Caused by the Occurrence of Spontaneous Local Ca^{2+} Release Events. Myotubes from WT and dysgenic mice exhibited similar very low rates of spontaneous local Ca^{2+} release events (LCRE) behavior (Fig. 6, *Left*). The occurrence of LCREs comprising Ca^{2+} sparks and macrospark release events (22) was similar despite the dysgenic myotubes having a significantly higher level of $[Ca^{2+}]_{rest}$ as estimated by the resting myofiber Fluo-4 fluorescence (Fig. 6, *Right*). After a 2-h incubation with 20 μM FK506, both WT and dysgenic myotubes showed a minor, nonsignificant increase in Ca^{2+} spark activity. On the other hand, in both groups, FK506 treatment resulted in a relatively large and significant increase in resting fluorescence, consistent with the results obtained when Ca^{2+}-selective microelectrodes were used (compare Figs. 1 and 6).

Discussion

It has been previously reported that the rate of passive Ca^{2+} release from SR vesicles is 10^3- to 10^4-fold smaller than the rate of active Ca^{2+} release in vivo and is likely to reflect passive Ca^{2+} flux from the SR in relaxed muscle. The comparison of the passive Ca^{2+} release rate in light and heavy SR fraction vesicles (LSR and HSR, respectively) shows that the rate in HSR is at least fourfold faster than in LSR membranes (23). This observation is in good agreement with the preferential location of RyR1 in the terminal cisternae of the SR and HSR vesicles, suggesting that RyR1 could be a significant contributor to the passive Ca^{2+} release from the SR. B5, an agent that directly interacts with RyR1, is able to reduce passive leak (18) and increase SR filling capacity (19). More direct evidence that supports the participation of RyR1 in the passive Ca^{2+} release from the SR and the control of $[Ca^{2+}]_{rest}$ in muscle cells is that when RyR1s bearing mutations that cause malignant hyperthermia are expressed in RyR1-null myotubes, the amount of Ca^{2+} release in response to caffeine is decreased (24, 25), and $[Ca^{2+}]_{rest}$ is in-

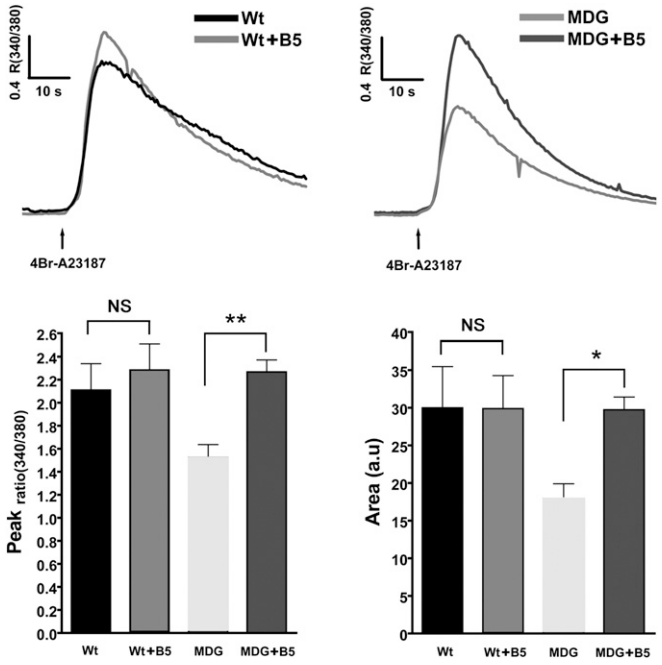

Fig. 5. Intracellular Ca^{2+} content is decreased in dysgenic myotubes and is corrected by B5. WT and dysgenic myotubes were loaded with the ratiometric dye Fura-4F. The total Ca^{2+} released by 4Br-A23187 in Ca^{2+}-free solution was measured as an estimation of the Ca^{2+}SR loading of the myotubes. Mean traces of the responses [WT black trace and dysgenic (MDG) trace] and the effect of 20 μM B5 are shown [WT+B5 trace and dysgenic (MDG)+B5 trace]. *Lower:* Graphs show peak and area values plotted as mean ± SEM [WT $n = 20$, dysgenic (MDG) $n = 29$, WT+B5 $n = 24$, dysgenic (MDG)+B5 $n = 15$]. $^{*}P < 0.05$; $^{**}P < 0.01$ (ANOVA).

creased compared with WT. In addition, B5 had a greater effect in decreasing $[Ca^{2+}]_{rest}$ in cells expressing malignant hyperthermia RyR1s than WT RyR1 (4), and the combined action of B5 and ryanodine on WT myotubes, which controls the RyR1 leak and blocks the channels at the same time, decreased $[Ca^{2+}]_{rest}$ to the same level as RyR1-null myotubes, which do not express any RyR isoform and are unresponsive to B5 and ryanodine treatment (10). In addition to RyR1, $Ca_V1.1$ is a locus for mutations

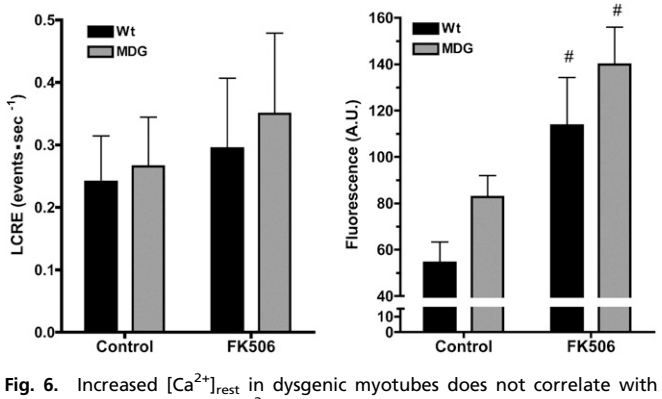

Fig. 6. Increased $[Ca^{2+}]_{rest}$ in dysgenic myotubes does not correlate with frequency of spontaneous Ca^{2+}sparks. Spontaneous LCREs were measured as described in *Materials and Methods* on WT and dysgenic (MDG) myotubes. The frequency of spontaneous LCRE was calculated for each individual cell, and the data are shown as mean ± SEM (*Left*; WT $n = 10$, dysgenic $n = 10$). In addition, the global fluorescence of each myotube was calculated and plotted (*Right*; WT $n = 10$, dysgenic $n = 10$) as mean ± SEM. $^{\#}P < 0.05$ (ANOVA). The effect of FK506 treatment on both LCRE frequency and global fluorescence is shown.

that cause the malignant hyperthermia syndrome (26–28). The mechanism by which DHPR structural alterations may affect RyR1 function to cause this syndrome is currently unknown. It is possible that the disruption of the unique orthograde communication described in this work may be a plausible explanation of how RyR1 leak is enhanced by these mutations, leading to the increase in $[Ca^{2+}]_{rest}$ that is a common feature of malignant hyperthermia susceptibility.

To demonstrate that the effect of B5 treatment was specific to reducing RyR1 leak and not due to a primary reduction of Ca^{2+} sarcolemmal entry, we showed that in WT and dysgenic myotubes that have had their SR Ca^{2+} stores depleted with thapsigargin, that application of B5 has no effect on Ca^{2+} entry (Fig. S1). Our results confirm the previous observations that B5 requires an intact RyR1–FKBP12 complex to stimulate the transition of RyR1 from the leak to a gating state because FK506 treatment almost completely blocked the action of B5 in all of the cell types tested. Thus, all of these data strongly suggest that the RyR1 leak is a normal component that is required for the maintenance of normal Ca^{2+} homeostasis in muscle. Interestingly, profound differences between WT and dysgenic myotubes in relation to leak channel activity at rest suggest an important role of DHPR in controlling RyR1s transitions between the gating and leak states. The pharmacological control of leak-RyR1s using B5 clearly shows that dysgenic cells have a higher proportion of leak-RyR1s than WT cells.

Under physiologic culture conditions cultured WT and dysgenic myotubes show Ca^{2+} sparks at very low frequency that are predominantly located in the central portion of the myotubes away from the peripheral regions where sarcolemma–SR couplings and partially developed t-tubules are found. However, spark frequency was differentially increased in dysgenic myotubes when the culture medium contains 1 mM caffeine and high Ca^{2+}. This led to the suggestion that the DHPR negatively regulates the spontaneous Ca^{2+} release through RyR1 (29). Support for this negative regulation comes from our discovery that when RyR3, which is not regulated by the DHPR, is expressed in dyspedic (RyR null) cells, spark frequency is high and $[Ca^{2+}]_{rest}$ is elevated (1, 22, 30). Our present results agree with the previous observations because we see no difference in the frequency or characteristics of spontaneous sparks between dysgenic and WT myotubes in standard resting conditions measured at 25 °C. Because sparks are not more frequent in dysgenic than WT, we believe that the increased $[Ca^{2+}]_{rest}$ in dysgenic myotubes can be accounted for by a greater proportion of RyR1s existing in a low-conductance leak state with high open probability, rather than to an increase in release events.

The constant repressive action by the presence of the DHPR on the transition of RyR1 into the leak state is very important not only to maintain normal $[Ca^{2+}]_{rest}$ in skeletal myotubes but to prevent depletion of the SR–Ca^{2+} content, as demonstrated by the fact that 20-min treatment with B5 is enough to restore normal SR Ca^{2+} loading in dysgenic myotubes. In this new equilibrium, because the SR–Ca^{2+} content is normal, the plasmalemmal Ca^{2+} permeability is low. Thus, these data suggest that the RyR1 leak controls the fine-tuning of the SR–Ca^{2+} content as well as maintaining $[Ca^{+2}]_{rest}$ constant within a tight homeostatic range (Fig. 7, *Left*). The absence of expression of $Ca_V1.1$ in dysgenic myotubes releases this orthograde repression of RyR1 transitions to the leak state and results in an increased passive Ca^{2+} efflux from the SR through RyR1. It has been suggested that, in resting condition, plasmalemmal Ca^{2+} permeability is constantly controlled by the Ca^{2+} content level in the SR, through a feedback mechanism that involves coordination between Stim1 and/or STIM2 in the SR and the highly Ca^{2+}-selective Orai1 channel (31). In muscle cells we recently have shown that Orai1-mediated resting Ca^{2+} entry accounts for approximately half of the basal entry and is sensitive to BTP2 (11).

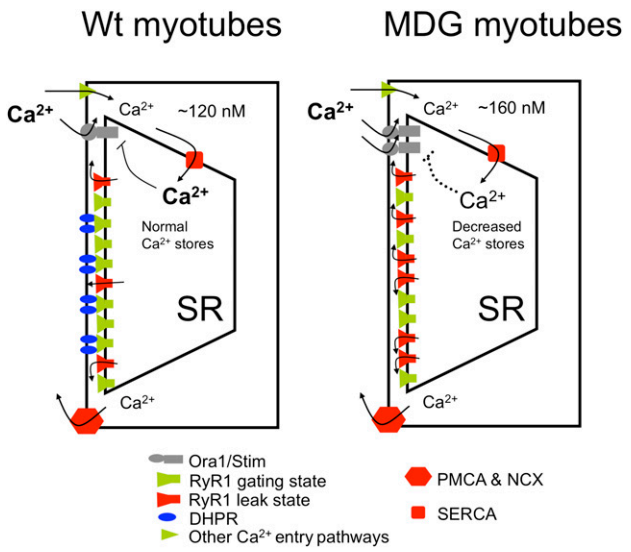

Fig. 7. Altered resting Ca^{2+} homeostasis in dysgenic (MDG) myotubes (a model). We propose a model in which association with the DHPR does not allow RyRs to enter into the leak state. This limits the availability of leaky channels and preserves a restricted passive Ca^{+2} efflux from the SR. At equilibrium the SR Ca^{2+} content is not depleted, and negative feedback controls the plasmalemmal Ca^{+2} permeability (*Left*). In the absence of DHPRs, in dysgenic (MDG) myotubes, there is an increased passive Ca^{2+} efflux from the SR through RyR1, resulting in an increase of $[Ca^{2+}]_{rest}$ and a decrease of Ca^{2+}content in the SR, thus activating store operated calcium entry. The overall effect is an increase of the $[Ca^{2+}]_{rest}$ (*Right*). SERCA, sarco-endoplasmic Ca^{2+} ATPase; PMCA, plasma membrane Ca^{2+} ATPase; NCX, Ca^{2+}/Na^{+} exchanger of the plasma membrane.

Thus, supporting the idea of an inverse relationship between SR Ca^{2+} load and plasmalemmal Ca^{2+} permeability at rest, dysgenic myotubes, which have decreased SR Ca^{2+} loading, showed 40% higher resting Ca^{2+} entry than WT myotubes (Fig. 7, *Right*), and BTP2 decreased $[Ca^{2+}]_{rest}$ more in dysgenic myotubes (37 nM decrement) than in WT (27 nM decrement). In contrast, in myotubes that have RyR1 leaks converted to gating channels with B5, where SR loading is equalized, the effect of BTP2 on $[Ca^{2+}]_{rest}$ is not different in dysgenic (19 nM decrement) and WT myotubes (20 nM decrement).

On the basis of the mechanism of orthograde coupling between RyR1 and DHPR reported here, the RyR1 population not physically associated with DHPRs should have an increased probability to be in the leak conformation. This observation suggests that the function of RyR1s that are not under direct control by a DHPR is to maintain a certain amount of SR leak to preserve physiologic $[Ca^{2+}]_{rest}$ and overall Ca^{2+} homeostasis at rest.

Materials and Methods

Determination of $[Ca^{2+}]_{rest}$. ***Ca^{2+}-selective microelectrodes.*** Double-barreled Ca^{2+}-selective microelectrodes were prepared and calibrated as previously described (32). Only those electrodes with a linear relationship between pCa3 and pCa8 (Nernstian response, 28.5 mV per pCa unit at 24 °C) were used experimentally. To better mimic the intracellular ionic conditions, all calibration solutions were supplemented with 1 mM Mg^{2+}. All electrodes were then recalibrated after making measurements of $[Ca^{2+}]_{rest}$, and if the two calibration curves did not agree within 3 mV from pCa7 to pCa8, the data from that microelectrode were discarded.

Recording of Vm and $[Ca^{2+}]_{rest}$. Myotubes were impaled with the double-barreled microelectrode, and potentials were recorded via high impedance amplifier (WPI FD-223). The potential from the 3M KCl barrel (Vm) was subtracted electronically from VCa_E, to produce a differential Ca^{2+}-specific potential (V_{Ca}) that represents the $[Ca^{2+}]_{rest}$. Vm and V_{Ca} were filtered (30–50 KHz) to improve the signal-to-noise ratio and stored in a computer for further analysis.

Lentiviral Transduction of Dysgenic Myoblasts. The $Ca_V1.1$ cDNA kindly provided by Manfred Grabner (33) was subcloned between the LTRs of a lentiviral vector driven by an EF1α human promoter. The lentiviral particles were packaged in HEK 293T cells according to a standard method (34). Dysgenic myoblasts were transduced with lentiviral particles and 24 h later were plated in one cell per well in a 96-well plate. After 2 to 3 wk, myoblasts from 20–30 clones were plated in 96-well imaging plates and differentiated to myotubes. After loading with Fluo-4 AM the myotubes were challenged to KCl depolarization. Cells expressing $Ca_V1.1$ showed strong Ca^{2+} transient in response to depolarization, whereas negative and uninfected dysgenic cells showed no signal. $Ca_V1.1$ expression and targeting in each clone was evaluated using Western blot and immunofluorescence. After 5 to 6 d of differentiation the cultures showed multinucleated myotubes, with clustering of DHPRs at the cell surface (evaluated by immunofluorescence).

Resting Ca^{2+} Entry. Fura-2–loaded myotubes were perfused with imaging solution [140 mM NaCl, 5 mM KCl, 1 mM $MgCl_2$, 1 mM $CaCl_2$, 5.5 mM glucose, and 10 mM Hepes (pH 7.4)] for 1 min and then the perfusion system switched to Mn^{2+}-containing solution [140 mM NaCl, 5 mM KCl, 0.5 mM $MnCl_2$, 5.5 mM glucose, 10 mM Hepes (pH 7.4), ≈7 μM Ca^{2+} (unbuffered nominally Ca^{2+} free buffer)] for 3 min. Some recordings showed motion artifact due to perfusion switching, and to minimize errors in calculating the rate of decrease in Fura-2 fluorescence after Mn^{2+} exposure, the rate was measured when the signal was linear and stable (30 s after solution twitching). To calculate the fluorescence quench rate, the stable part of the signal was fitted to a linear regression (y = a + bx). The slope derived is expressed as fluorescence arbitrary units per second (f.a.u/s). The excitation wavelength used to measure Mn^{2+} quench of Fura-2 was monitored using a 357/7-nm excitation and 510/80-nm emission filter.

Sarcoplasmic Reticulum Ca^{2+} Content. Myotubes preparations were loaded with 5 μM Fluo-5N AM for 20 min at 37 °C. The myotubes were placed on the stage of an epifluorescence microscope (Nikon TE2000) coupled to a digital acquisition system (Stanford Photonics). The filter set used was excitation 480/30 nm and emission 535/40 nm. The emission signal was acquired at a frequency of 30 frames per second. The amount of SR Ca^{2+} was estimated by taking the area under the curve of the signal induced by 20 mM caffeine in nominally Ca^{2+}-free media [140 mM NaCl, 5 mM KCl, 2 mM $MgCl_2$, 5.5 mM glucose, 1 mM EGTA, 10 mM Hepes (pH 7.4), ≈5 nM free Ca^{2+}] to minimize Ca^{2+} entry. To estimate the total amount of Ca^{2+} stored in the intracellular compartments, ratiometric Ca^{2+} sensor Fura-4F AM loaded myotubes were exposed to the Ca^{2+} ionophore 4Br-A23187 in Ca^{2+}-free media buffered with 1 mM EGTA. The area under the curve and the peak of Ca^{2+} transient were computed for each myotube genotype studied. Fluorescent emission at 510 nm was captured from regions of interest within each myotube at two frames per second and expressed as ratio between 340-nm and 380-nm excitation wavelengths.

Western Blot and Immunofluorescence. Membrane vesicles were prepared from differentiated myotubes by homogenizing them in a Polytron cell disrupter in buffer containing 5 mM imidazole (pH 7.4) and 300 mM sucrose supplemented with protease inhibitor (Complete, Roche Applied Science) and collected as previously described (1). Proteins were separated using SDS/PAGE and transferred to polyvinylidene difluoride membranes. Expression of specific proteins was assessed by incubation of the membranes with monoclonal antibodies against RyR (34C, Developmental Studies Hybridoma Bank) or $Ca_V1.1$ (MA3-920, ABR-Affinity BioReagents). For immunofluorescence localization of $Ca_V1.1$, differentiated myotubes were fixed in cold methanol for 15 min at −20 °C. Cells were rinsed with PBS, then were blocked for nonspecific interactions with PSB-1% BSA for 1 h at room temperature and incubated overnight with anti-$Ca_V1.1$ monoclonal antibody at a 1:400 dilution at 4 °C. Cells were washed and then incubated for 1 h with Alexa Fluor-514 goat anti-mouse antibody (Invitrogen). DAPI was used for nuclear visualization.

LCRE Activity (Ca^{2+} Sparks). Myotubes grown in 96-well special optics plates (Corning) were loaded with the Ca^{2+} indicator dye Fluo-4 AM (Teflabs) as previously described (22). Plates were mounted over an inverted confocal fluorescence microscope system (Zeiss LIVE5; 25×, 0.8 NA H_20 objective) and fields of myotubes (193.9 μm in *x* and *y*) were imaged (30 Hz; 6–8 s) using *x/y* scanning. Image series were analyzed with custom routines (IDL; Kodak) for spontaneous LCRE activity as previously described (22, 35, 36).

Isolation of B5. B5 was extracted from lyophilized *Ianthella basta* sponge collected from Guam using previously described methods (19).

Statistics. All values are expressed as mean ± SEM. Statistical analysis was performed using one-way analysis of variance and Tukey's posttest for multiple measurements to determine significance ($P < 0.05$).

ACKNOWLEDGMENTS. We thank Dr. Claudio Perez and Mr. John Szypt for their assistance with Ca^{2+} imaging and preparation of Fig. S1; Dr. Karen Westerman for dihydropyridine receptor subcloning and for setting up the lentiviral transduction procedure for myoblasts; and Dr. Peter Schupp for the gift of *Ianthella basta*. This work was supported by National Institutes of Health Grants 2R01AR43140 and 5P01 AR052354 (to P.D.A. and I.N.P.).

1. Perez CF, López JR, Allen PD (2005) Expression levels of RyR1 and RyR3 control resting free Ca2+ in skeletal muscle. *Am J Physiol Cell Physiol* 288:C640–C649.
2. Berridge MJ, Bootman MD, Roderick HL (2003) Calcium signalling: Dynamics, homeostasis and remodelling. *Nat Rev Mol Cell Biol* 4:517–529.
3. Turner PR, Westwood T, Regen CM, Steinhardt RA (1988) Increased protein degradation results from elevated free calcium levels found in muscle from mdx mice. *Nature* 335:735–738.
4. Yang T, et al. (2007) Elevated resting [Ca(2+)](i) in myotubes expressing malignant hyperthermia RyR1 cDNAs is partially restored by modulation of passive calcium leak from the SR. *Am J Physiol Cell Physiol* 292:C1591–C1598.
5. Lopez JR, Gerardi A, Lopez MJ, Allen PD (1992) Effects of dantrolene on myoplasmic free [Ca2+] measured in vivo in patients susceptible to malignant hyperthermia. *Anesthesiology* 76:711–719.
6. Moussa CE, et al. (2006) Transgenic expression of beta-APP in fast-twitch skeletal muscle leads to calcium dyshomeostasis and IBM-like pathology. *FASEB J* 20: 2165–2167.
7. Christensen RA, Shtifman A, Allen PD, Lopez JR, Querfurth HW (2004) Calcium dyshomeostasis in beta-amyloid and tau-bearing skeletal myotubes. *J Biol Chem* 279: 53524–53532.
8. Martonosi AN (1984) Mechanisms of Ca2+ release from sarcoplasmic reticulum of skeletal muscle. *Physiol Rev* 64:1240–1320.
9. Ríos E (2010) The cell boundary theorem: A simple law of the control of cytosolic calcium concentration. *J Physiol Sci* 60:81–84.
10. Eltit JM, et al. (2010) RyR1-mediated Ca2+ leak and Ca2+ entry determine resting intracellular Ca2+ in skeletal myotubes. *J Biol Chem* 285:13781–13787.
11. Li H, et al. (2010) Impaired Orai1-mediated resting Ca2+ entry reduces the cytosolic [Ca2+] and sarcoplasmic reticulum Ca2+ loading in quiescent junctophilin 1 knock-out myotubes. *J Biol Chem* 285:39171–39179.
12. Rios E (2010) RyR1 expression and the cell boundary theorem. *J Biol Chem* 285:le13; author reply le14.
13. Eltit JM, Perez C, Pessah IN, Allen PD, Lopez JR (2010) Reply to Rios: Cell boundary theorem and Ca2+ fluxes in skeletal muscle. *J Biol Chem* 285:le14.
14. Nakai J, et al. (1996) Enhanced dihydropyridine receptor channel activity in the presence of ryanodine receptor. *Nature* 380:72–75.
15. Franzini-Armstrong C, Kish JW (1995) Alternate disposition of tetrads in peripheral couplings of skeletal muscle. *J Muscle Res Cell Motil* 16:319–324.
16. Takekura H, Bennett L, Tanabe T, Beam KG, Franzini-Armstrong C (1994) Restoration of junctional tetrads in dysgenic myotubes by dihydropyridine receptor cDNA. *Biophys J* 67:793–803.
17. Protasi F, Franzini-Armstrong C, Allen PD (1998) Role of ryanodine receptors in the assembly of calcium release units in skeletal muscle. *J Cell Biol* 140:831–842.
18. Pessah IN, et al. (1997) Bastadins relate ryanodine-sensitive and -insensitive Ca2+ efflux pathways in skeletal SR and BC3H1 cells. *Am J Physiol* 272:C601–C614.
19. Mack MM, Molinski TF, Buck ED, Pessah IN (1994) Novel modulators of skeletal muscle FKBP12/calcium channel complex from Ianthella basta. Role of FKBP12 in channel gating. *J Biol Chem* 269:23236–23249.
20. Protasi F, Franzini-Armstrong C, Flucher BE (1997) Coordinated incorporation of skeletal muscle dihydropyridine receptors and ryanodine receptors in peripheral couplings of BC3H1 cells. *J Cell Biol* 137:859–870.
21. He LP, Hewavitharana T, Soboloff J, Spassova MA, Gill DL (2005) A functional link between store-operated and TRPC channels revealed by the 3,5-bis(trifluoromethyl) pyrazole derivative, BTP2. *J Biol Chem* 280:10997–11006.
22. Ward CW, et al. (2001) Type 1 and type 3 ryanodine receptors generate different Ca(2+) release event activity in both intact and permeabilized myotubes. *Biophys J* 81:3216–3230.
23. Watras J, Katz AM (1984) Calcium release from two fractions of sarcoplasmic reticulum from rabbit skeletal muscle. *Biochim Biophys Acta* 769:429–439.
24. Tong J, McCarthy TV, MacLennan DH (1999) Measurement of resting cytosolic Ca2+ concentrations and Ca2+ store size in HEK-293 cells transfected with malignant hyperthermia or central core disease mutant Ca2+ release channels. *J Biol Chem* 274: 693–702.
25. Yang T, Ta TA, Pessah IN, Allen PD (2003) Functional defects in six ryanodine receptor isoform-1 (RyR1) mutations associated with malignant hyperthermia and their impact on skeletal excitation-contraction coupling. *J Biol Chem* 278:25722–25730.
26. Weiss RG, et al. (2004) Functional analysis of the R1086H malignant hyperthermia mutation in the DHPR reveals an unexpected influence of the III-IV loop on skeletal muscle EC coupling. *Am J Physiol Cell Physiol* 287:C1094–C1102.
27. Pirone A, et al. (2010) Identification and functional characterization of malignant hyperthermia mutation T1354S in the outer pore of the Cavalpha1S-subunit. *Am J Physiol Cell Physiol* 299:C1345–C1354.
28. Carpenter D, et al. (2009) The role of CACNA1S in predisposition to malignant hyperthermia. *BMC Med Genet* 10:104.
29. Zhou J, et al. (2006) A probable role of dihydropyridine receptors in repression of Ca2+ sparks demonstrated in cultured mammalian muscle. *Am J Physiol Cell Physiol* 290:C539–C553.
30. Ward CW, et al. (2000) Expression of ryanodine receptor RyR3 produces Ca2+ sparks in dyspedic myotubes. *J Physiol* 525:91–103.
31. Brandman O, Liou J, Park WS, Meyer T (2007) STIM2 is a feedback regulator that stabilizes basal cytosolic and endoplasmic reticulum Ca2+ levels. *Cell* 131:1327–1339.
32. López JR, Contreras J, Linares N, Allen PD (2000) Hypersensitivity of malignant hyperthermia-susceptible swine skeletal muscle to caffeine is mediated by high resting myoplasmic [Ca2+]. *Anesthesiology* 92:1799–1806.
33. Grabner M, Dirksen RT, Beam KG (1998) Tagging with green fluorescent protein reveals a distinct subcellular distribution of L-type and non-L-type Ca2+ channels expressed in dysgenic myotubes. *Proc Natl Acad Sci USA* 95:1903–1908.
34. Westerman KA, Penvose A, Yang Z, Allen PD, Vacanti CA (2010) Adult muscle 'stem' cells can be sustained in culture as free-floating myospheres. *Exp Cell Res* 316: 1966–1976.
35. Iribe G, et al. (2009) Axial stretch of rat single ventricular cardiomyocytes causes an acute and transient increase in Ca2+ spark rate. *Circ Res* 104:787–795.
36. Lehnart SE, et al. (2008) Leaky Ca2+ release channel/ryanodine receptor 2 causes seizures and sudden cardiac death in mice. *J Clin Invest* 118:2230–2245.